Defect and Diffusion Forum
ISSN: 1662-9507, Vol. 451, pp 95-101
doi:10.4028/p-Is2sE9

Submitted: 2026-01-19
Revised: 2026-02-26
Accepted: 2026-03-01
Online: 2026-04-17

Material Characterization and Constitutive Modeling of PMMA for the Numerical Simulation of Vacuum Forming Process

Hyunsung Choi[1,a*], Minjae Baek[1,b], Yong Nam Kwon[1,c], Ducksung Kim[2,d], Daeho Jeong[2,e] and Yoo In Jeong[2,f]

[1]Aerospace research center, Korea Institute of Material Science, Changwon, South Korea

[2]Korea Aerospace Industries LTD., Sacheon, South Korea

[a*]h.choi@kims.re.kr, [b]qoralswo12@kims.re.kr, [c]kyn1740@kims.re.kr, [d]ducksung.kim@koreaaero.com, [e]daeho.jeong@koreaaero.com, [f]freud197@koreaaero.com

Keywords: PMMA, viscoplastic model, creep model, vacuum forming.

Abstract. In this study, the thermomechanical behavior of PMMA(poly-methyl methacrylate) during high-temperature vacuum forming was analyzed through both experimental and computational approaches. The material behavior of PMMA was modeled as a temperature and strain-rate dependent viscoplastic response, coupled with time-dependent creep deformation. The creep behavior was represented by the Norton–Bailey power law (Eq. 1), while the constitutive model for the strain rate and temperature-dependent stress-strain behavior was implemented in ABAQUS via a user subroutine (UHARD). The forming process was simulated by using ABAQUS/Standard VISCO solver, incorporating vacuum pressure loading and clamping conditions. The numerical framework enables effective analysis of deformation behavior under thermomechanical forming conditions and provides a basis for process-oriented modeling of PMMA vacuum forming.

Introduction

Stretched acrylic has widely adopted as a transparent material for fighter jet canopy components due to its excellent optical transmittance, impact resistance, weatherability, and thermal stability. Transparent aircraft components are commonly fabricated through vacuum forming of PMMA sheets at elevated temperatures below the glass transition temperature. However, the vacuum forming process is highly sensitive to process parameters such as temperature, forming time, vacuum pressure, and clamping conditions, which strongly influence thickness uniformity and residual stress distribution in the final product.

To ensure process reliability and to reduce costly trial-and-error during PMMA forming, accurate material characterization and reliable finite element (FE) modeling are essential [1,2]. Among the various factors affecting numerical accuracy, appropriate representation of material behavior plays a critical role in thermomechanical forming simulations. Polymer material behavior can be effectively incorporated into FE simulations through constitutive modeling that accounts for temperature, strain rate, and time-dependent deformation.

Previous studies have investigated the mechanical behavior of transparent polymers such as PMMA and polycarbonate (PC), highlighting the brittle response of PMMA in contrast to the ductile behavior of PC [3]. The effects of temperature, stress, and crazing on creep life have also been reported [4], and stress-relaxation behavior of PMMA across the glass transition temperature has been characterized with corresponding constitutive models [5]. In addition, large-strain springback behavior of PMMA has been experimentally investigated and numerically predicted using finite element approaches [6]. Rate-dependent constitutive models have been proposed to describe strain-rate sensitivity [7], and large-strain mechanical behavior of PMMA at elevated temperatures has been examined through uniaxial compression testing [8].

In this work, the temperature- and strain-rate-dependent stress–strain behavior, along with the creep response of PMMA, was characterized through uniaxial tensile testing.

Viscoplastic and creep constitutive models were adopted to represent the observed material behavior, and the corresponding material parameters were identified based on experimental results.
Finite element simulation of the vacuum forming process for a double-ellipsoidal transparent component was performed using the ABAQUS/Standard VISCO solver.

Material Characterization

Uniaxial tensile specimen was performed with temperature of 80, 90, and 100℃ and strain rate of 0.001/s and 0.01/s. Specimens were machined from a 7 mm-thick PMMA sheet in accordance with Type I geometry specified in ASTM D638-22, as shown in Fig. 1 and summarized in Table 1. Strain was measured using a 3D Digital Image Correlation (DIC) technique to accurately capture the large deformation behavior at elevated temperatures, as illustrated in Fig. 2. To ensure repeatability and reproducibility, each test condition was repeated three times. The results of uniaxial tensile test with respect to different temperature level and strain rate range are plotted in Fig. 3 where Fig. 3a indicates test results for the temperature of 80, 90, and 100℃ at strain rate of 0.001/s and Fig. 3b is the results for the temperature of 80, 90, and 100℃ at strain rate of 0.01/s. As shown in the figures, the flow stress decreases with increasing temperature. In addition, the material exhibits positive strain-rate sensitivity, indicating an increase in flow stress with increasing strain rate.

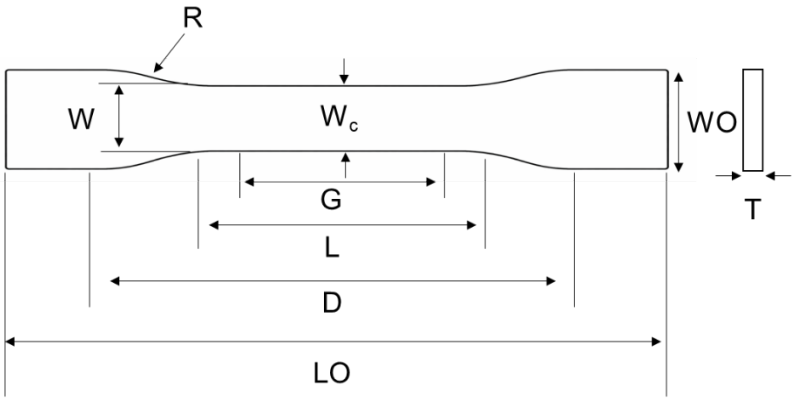

Fig. 1. Specimen geometry (ASTM D638-22).

Table 1. Dimension of uniaxial tensile specimen (ASTM D638-22).

W-Width of narrow section [mm]	L-Length of narrow section [mm]	WO-width overall [mm]	LO-length overall [mm]	G-Gage length [mm]	D-Distance between grips [mm]	R-Radius of fillet [mm]
13	57	19	165	50	115	76

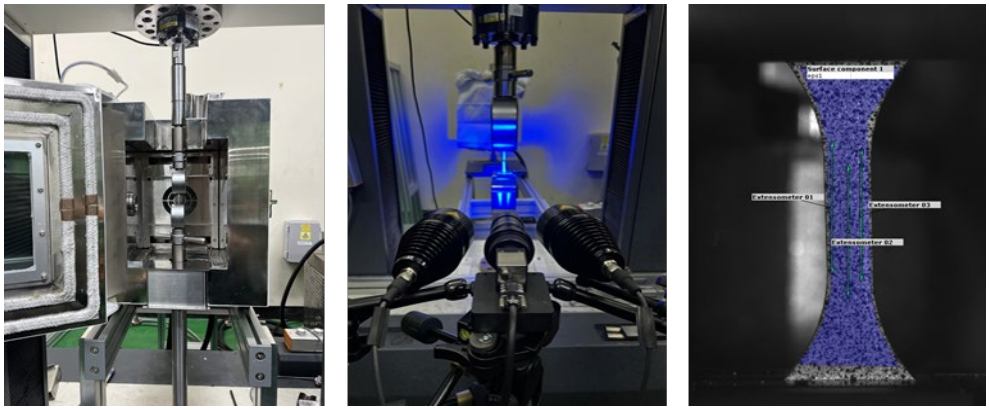

Fig. 2. Strain measurement by using Digital Image Correlation.

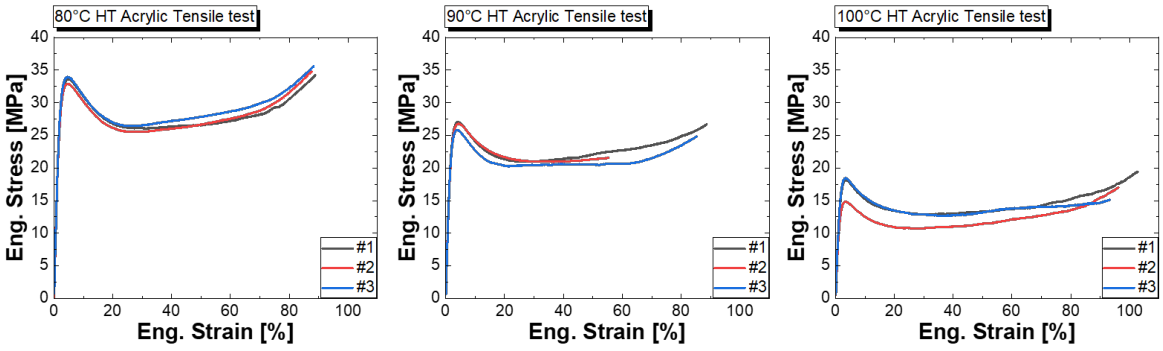

(a)

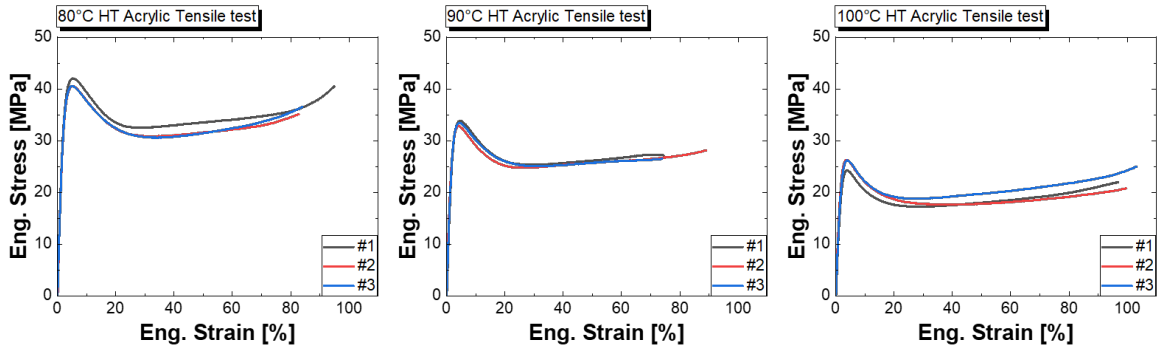

(b)

Fig. 3. Stress-strain behavior of PMMA for the temperature of 80, 90, and 100°C at the strain rate of (a) 0.001/s and (b) 0.01/s.

For creep characterization, the specimen geometry and experimental setup are shown in Fig. 4(a). Strain measurement was performed using a digital image correlation (DIC) system, consistent with the methodology adopted in the uniaxial tensile tests. Creep tests were conducted under a constant applied stress of 17 MPa at a temperature of 110 °C. The resulting creep strain–time response is presented in Fig. 4(b). As shown in the figure, the material exhibits an initial primary creep stage followed by a steady-state secondary creep regime, eventually leading to sudden fracture.

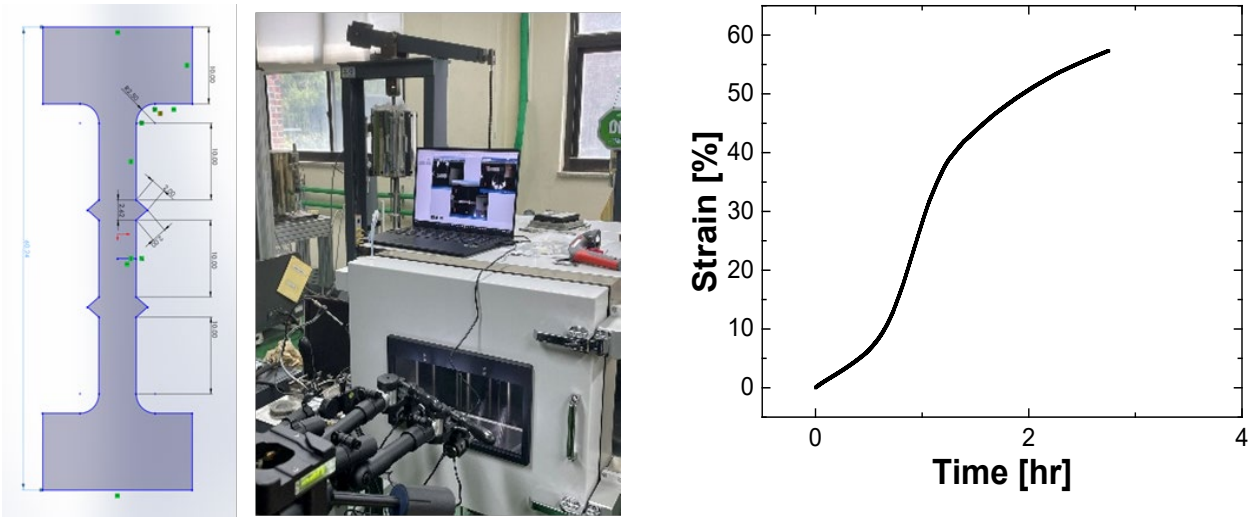

(a) (b)

Fig. 4. (a) Specimen geometry and equipment setup for creep test and (b) test results at stress of 17 MPa and temperature of 110 °C.

Constitutive Modeling

To describe the temperature- and strain-rate-dependent stress–strain behavior of PMMA, a constitutive model formulated in a multiplicative form was adopted [9], following the pioneering work of G'sell and Jonas [10]. This modeling framework enables effective representation of the coupled effects of temperature and strain rate on polymer deformation behavior under thermomechanical loading conditions.

$$\sigma_{eq}(\varepsilon,\dot{\varepsilon},T) = (1-\frac{T}{T_g})(1-\exp(-w\varepsilon)[\sigma_1 \exp(-b\varepsilon)(\frac{\dot{\varepsilon}}{\dot{\varepsilon}_{01}})^{m_1} + \sigma_2 \exp((h_0 + h_1 \frac{T-T_{ref}}{T_{ref}})(\varepsilon^2))(1+(\frac{\dot{\varepsilon}}{\dot{\varepsilon}_{02}})^{-1})^{-m_2}] \quad (1)$$

where T, T_g, and T_{ref} denote the absolute, glass transition, and reference temperature, respectively. ε represents true strain, while $\dot{\varepsilon}, \dot{\varepsilon}_{01}$, and $\dot{\varepsilon}_{02}$ correspond to the current and reference strain rate, respectively. In addition, the parameters of $w, b, h_0, m_1, m_2, \sigma_1$, and σ_2 are material coefficients that need to be identified by fitting with experimental results of strain rate and temperature-dependent stress-strain behavior. The identified material parameters are summarized in Table 2 which are identified by optimization process that minimizes error between experimental and predicted stress-strain responses, and the predicted temperature- and strain-rate-dependent stress–strain behavior is compared with experimental results in Fig. 5. Although the model captures the overall trends of strain-rate and temperature dependency, its predictive accuracy remains limited. In particular, the material softening at elevated temperatures is overestimated. Furthermore, the saturation behavior observed at large strains is not adequately reproduced, indicating the necessity for further development of the constitutive model to achieve more accurate representation of PMMA deformation behavior.

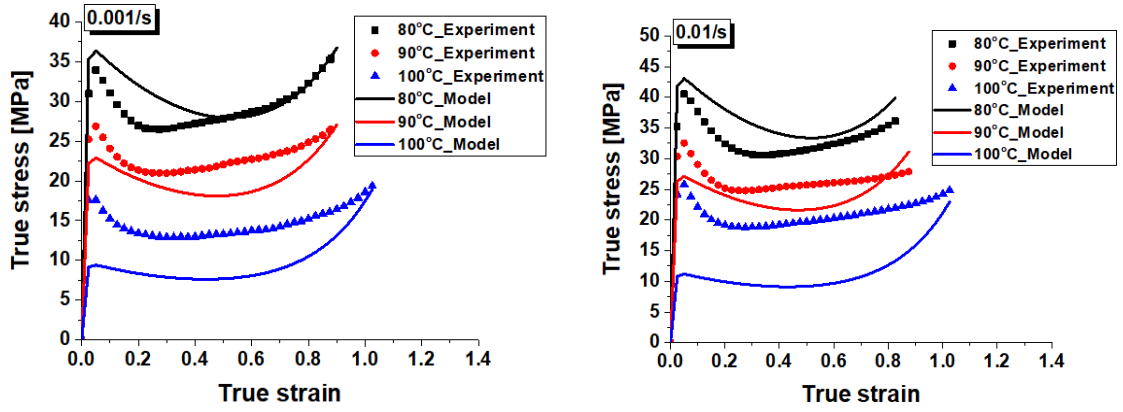

(a) (b)

Fig. 5. Predicted Stress-strain behavior by the constitutive model [9]: (a) 0.001/s and (b) 0.01/s.

Table 2. Material coefficients of the constitutive model [9].

T_g [K]	T_{ref} [K]	σ_1 [MPa]	σ_2 [MPa]	b	h_0	h_1
393	298	409.695	162.040	1.321	1.129e-7	7.438
m_1	m_2	$\dot{\varepsilon}_{01}$ [1/s]	$\dot{\varepsilon}_{02}$ [1/s]	w		
0.700	0.330	0.001	0.001	116.056		

To account for the creep behavior of PMMA, the time–power law creep model implemented in ABAQUS was adopted, as expressed in Eq. (2):

$$\dot{\varepsilon}_c = \dot{\varepsilon}_0 \left(\frac{\bar{\sigma}}{\bar{\sigma}_0} \right)^n (\dot{\varepsilon}_o t)^m \tag{2}$$

where $\dot{\varepsilon}_c, t$, and $\bar{\sigma}$ denote creep strain rate, time, and effective stress, respectively. In addition, $\bar{\sigma}_0$ is reference effective stress. $\dot{\varepsilon}_0, n$, and m are material coefficients need to be identified with creep test results. The identified creep material parameters are summarized in Table 3, and the predicted creep behavior is compared with experimental results in Fig. 6. The model shows good agreement with the experimental data, particularly in capturing the primary and secondary creep regions.

Table 3. Material coefficients of time-power law.

$\dot{\varepsilon}_0$	n	m	$\bar{\sigma}_0$ [MPa]
9.823e-3	0.594	-0.293	10

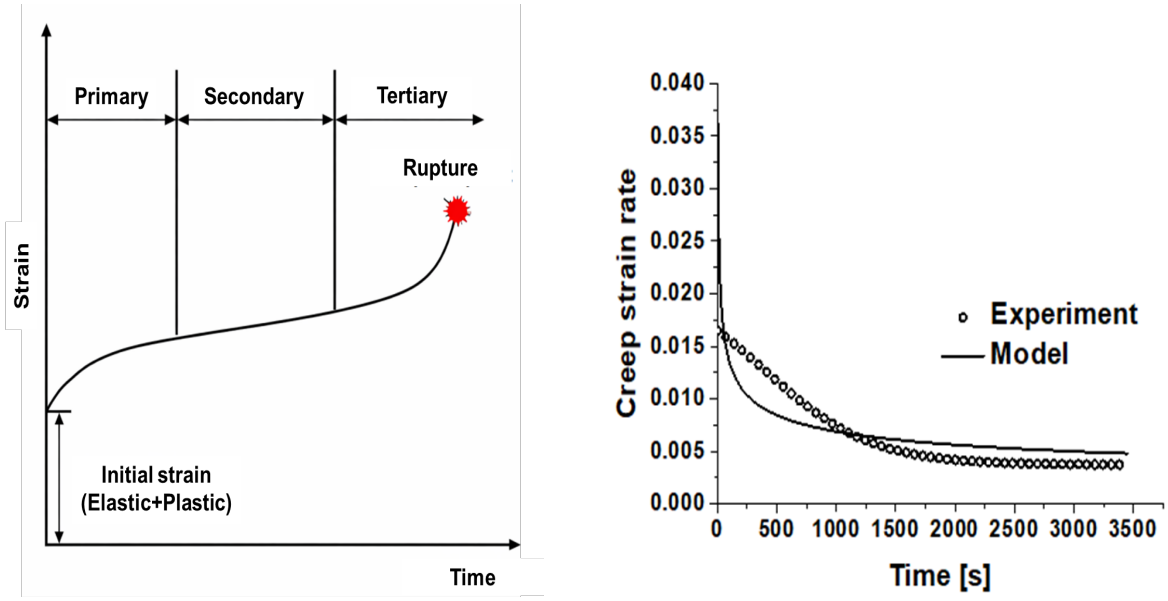

(a) (b)

Fig. 6. (a) Region of creep behavior and (b) predicted creep behavior by time-power law.

Finite Element Simulation of Vacuum Forming

The vacuum forming process of a double-ellipsoidal component was simulated using ABAQUS/Standard with the VISCO solver. The forming die was modeled as a rigid body, while the PMMA sheet was modeled as a deformable body using three-dimensional solid elements. As shown in Fig. 7, the outer region of the PMMA sheet was fully constrained to represent the clamping condition. In addition, symmetry boundary conditions were applied to improve computational efficiency. A uniform temperature of 100 °C was imposed on the material, and a Coulomb friction coefficient of 0.2 was assumed between the die and the PMMA sheet. In the present simulation, heat transfer effects were neglected; therefore, the material temperature remained constant throughout the forming process. Vacuum pressure of 0.1 MPa was applied to the bottom surface of the PMMA sheet to drive the forming process.

The deformed shapes obtained from the vacuum forming simulation are shown in Fig. 8(a) and Fig. 8(b) for the front and side views, respectively. The results demonstrate that the double-ellipsoidal geometry can be effectively formed through the vacuum forming process. Notably, the vacuum forming is mainly based on creep deformation and maximum creep strain exceeds 0.8 which is concentrated near the top region of the formed component. This observation indicates that forming time and pressure control is a critical factor in the vacuum forming process of double-ellipsoidal PMMA components.

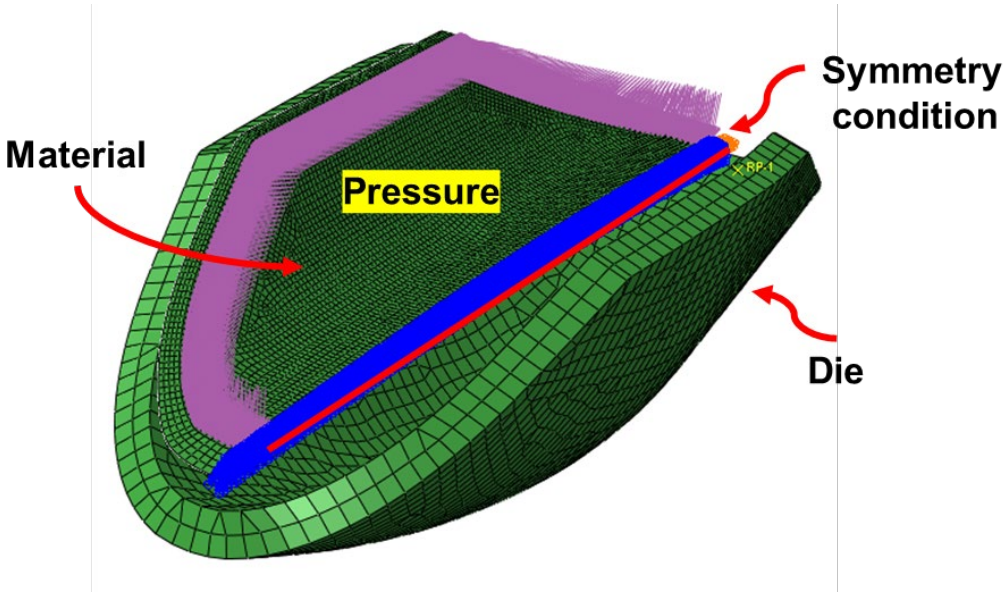

Fig. 7. Boundary conditions for the vacuum forming process.

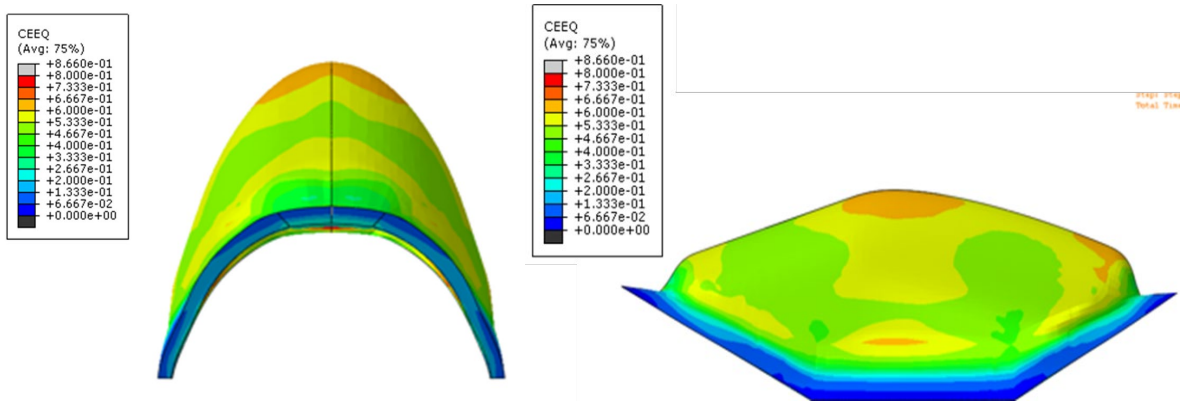

Fig. 8. The effective creep strain results of vacuum forming: (a) front view and (b) side view.

Conclusion

This study presented an experimental and numerical investigation of the thermomechanical behavior of PMMA during high-temperature vacuum forming. Temperature- and strain-rate-dependent stress–strain behavior, along with creep deformation, was characterized through uniaxial tensile and creep tests, and corresponding constitutive models were identified based on experimental data. The viscoplastic constitutive model captured the overall trends of temperature and strain-rate dependency, although limitations were observed in describing high-temperature softening and large-strain saturation behavior. In contrast, the time–power law creep model showed good agreement with experimental results, particularly in the primary and secondary creep regimes. Finite element simulation of the vacuum forming process using the ABAQUS/Standard VISCO solver demonstrated that the double-ellipsoidal PMMA component could be effectively formed. The results further revealed that large creep strains develop near the top region of the component, highlighting the critical importance of forming time and pressure control in vacuum forming of complex PMMA geometries.

References

[1] Dong, Y., R. J. T. Lin, and D. Bhattacharyya. "Finite element simulation on thermoforming acrylic sheets using dynamic explicit method." Polymers and Polymer Composites 14.3 (2006): 307-328.

[2] Azdast, Taher, et al. "Numerical and experimental analysis of wall thickness variation of a hemispherical PMMA sheet in thermoforming process." The International Journal of Advanced Manufacturing Technology 64.1 (2013): 113-122.

[3] Tang, Zhiye, Kazushi Fujimoto, and Susumu Okazaki. "A comparison of the brittle PMMA with the ductile PC on the elasticity and yielding from a molecular dynamics perspective." Polymer 226 (2021): 123809.

[4] Gao, Zongzhan, et al. "Creep life assessment craze damage evolution of polyethylene methacrylate." Advances in Polymer Technology 37.8 (2018): 3619-3628.

[5] Mathiesen, Danielle, Dana Vogtmann, and Rebecca B. Dupaix. "Characterization and constitutive modeling of stress-relaxation behavior of Poly (methyl methacrylate)(PMMA) across the glass transition temperature." Mechanics of Materials 71 (2014): 74-84.

[6] Mathiesen, D., A. Kakumani, and R. B. Dupaix. "Experimental Characterization and Finite Element Prediction of Large Strain Spring-Back Behavior of Poly (Methyl Methacrylate)." Journal of Engineering Materials and Technology 141.3 (2019): 031005.

[7] Mulliken, Adam D., and Mary C. Boyce. "Mechanics of the rate-dependent elastic–plastic deformation of glassy polymers from low to high strain rates." International journal of solids and structures 43.5 (2006): 1331-1356.

[8] Palm, G., R. B. Dupaix, and J. Castro. "Large strain mechanical behavior of poly (methyl methacrylate)(PMMA) near the glass transition temperature." (2006): 559-563.

[9] Nasraoui, M., et al. "Influence of strain rate, temperature and adiabatic heating on the mechanical behaviour of poly-methyl-methacrylate: Experimental and modelling analyses." Materials & Design 37 (2012): 500-509.

[10] G'sell, Ch, and J. J. Jonas. "Determination of the plastic behaviour of solid polymers at constant true strain rate." Journal of materials science 14.3 (1979): 583-591.